

MAGNETOPLASMAIONIC (MPI) ENGINE

Naveen Kumar Chaudhary[1]
[1]Independent Researcher, Perth, Western Australia, Australia

Abstract

The Magnetoplasmaionic (MPI) Engine may represent a transformative approach to propulsion technology by utilizing Earth's atmospheric electricity as a primary energy source. Unlike conventional chemical propulsion systems that depend on stored fuels, the MPI Engine can harvest naturally occurring ions and plasma from the atmosphere and accelerate them using electromagnetic forces. This concept may eliminate fuel dependency, enabling continuous operation powered by renewable atmospheric energy and aligning with global sustainability objectives. The MPI Engine design can operate on the Lorentz force principle, accelerating plasma within a controlled magnetic confinement system. Its architecture may integrate advanced superconducting magnetic coils, multistage ionization processes, and precision electrode configurations to achieve efficient plasma acceleration. Atmospheric energy collection can be facilitated through carbon based materials and corona discharge systems, which concentrate and channel ionized particles into the engine for propulsion. Adaptive control systems may optimize performance under varying environmental conditions, ensuring operational stability and safety. Materials science can play a critical role in the MPI Engine's design, with ultra high temperature ceramics and advanced cathode technologies providing resilience against extreme thermal and electromagnetic stresses. Comprehensive safety protocols, including rapid shutdown mechanisms and electromagnetic shielding, may ensure compliance with international standards for functional safety and environmental protection. Studies can demonstrate the MPI Engine's capability to deliver high thrust efficiency and operational reliability, while its modular design may support scalability for diverse applications. Initially developed for high speed terrestrial transportation systems, the technology can also offer significant potential for aerospace and maritime domains, providing a versatile solution for next generation mobility.

By combining plasma physics, atmospheric energy harvesting, and advanced engineering principles, the MPI Engine may redefine propulsion paradigms. Its ability to deliver high performance without emissions can position it as a transformative technology for sustainable transportation, paving the way for cleaner, more efficient mobility solutions in the future.

Keywords: Atmospheric Energy Propulsion, Plasma Acceleration, Sustainable Transportation, Advanced Propulsion Systems

1. Introduction

Sustainable high performance propulsion is a defining challenge for the next generation of aeronautical and ground transport systems. Conventional chemical propulsion systems combust stored fuels, producing greenhouse gases and requiring continuous logistical supply chains. Electric

https://doi.org/10.71945/icas2026_0739

propulsion, initially developed for spacecraft, offers high specific impulse but depends on carried propellants (typically xenon or krypton) and is designed for vacuum conditions [5]. No currently operational terrestrial or atmospheric propulsion concept exploits the naturally available ionised atmospheric medium near Earth's surface as a working fluid [3], [4].

The MPI Engine is proposed as a theoretical propulsion architecture intended to explore the interaction between atmospheric ionization processes and electromagnetic plasma acceleration mechanisms within near atmospheric operating environments [2], [3], [5]. The Magnetoplasmaionic (MPI) Engine is proposed as a conceptual propulsion approach that explores the use of atmospheric ionisation and electromagnetic acceleration mechanisms. It is conceived as a propulsion system that collects atmospheric ions and electrons, augments their density through corona discharge and active ionisation, confines the resulting plasma using superconducting magnetic fields, and accelerates the plasma through electromagnetic Lorentz force interaction to produce directed thrust [2], [4], [5], [6]. Because the working mass is drawn from the ambient atmosphere rather than a tank, the system proposes a pathway toward propellant supplemented propulsion [2]. The MPI Engine concept has been developed primarily within the Ringway Transportation System, a proposed high speed, pillar supported, magnetically levitated transport network [1], [2], [8] but its physical basis is general enough to apply to low altitude atmospheric flight vehicles and future hybrid aerospace propulsion platforms [2], [5], [6]. The MPI Engine was conceived as the primary longitudinal propulsion element of the Ringway Transportation System is a novel high speed guideway in which vehicles travel through a succession of ring shaped frames mounted on spaced pillars, levitated and guided by superconducting magnets, and propelled by MPI thrust supplemented by iron cored long stator linear synchronous motors (LSMs) [1], [2], [7], [8]. The Ringway concept addresses urban transit congestion by providing an elevated or underground corridor that does not interfere with existing surface infrastructure [1], [2], [8]. Each Ringway pillar is equipped with an atmospheric energy collection subsystem arrays of carbon fibre, graphite, and graphene 'energy nails' and 'energy fibres' that concentrate the ambient atmospheric electric field, initiate corona discharge, and accumulate a localised energy cloud of ions and electrons in the passage through which the vehicle travels [1], [2], [3], [4]. As the vehicle passes through this cloud at operating speed, its nose mounted air intake duct draws in the enriched ion mixture and delivers it to the MPI Engine mounted on top of the vehicle fuselage [1], [2].

1.1 Objective

This paper has objectives: (i) introduce the physical foundations of atmospheric electricity, corona discharge, and Lorentz force propulsion that underpin the MPI Engine concept; (ii) describe the MPI Engine architecture, including primary configuration components; (iii) define the operational mode; (iv) detail prospective materials selection, thermal management, and structural integrity requirements; and (v) describe the Ringway Infrastructure interface.

2. Physical Foundations

2.1 Earth’s Atmospheric Electric Environment

The global atmospheric electric circuit maintains a potential difference of approximately 250 to 300 kV between the ionosphere and Earth's surface, driven by global thunderstorm activity and sustained by fair weather conduction currents of order 1 to 2 kA distributed globally [3], [4]. This circuit generates a fair weather electric field of approximately 100 to 300 V/m near the surface that diminishes with altitude and supports a continuous population of positive and negative small ions whose density ranges from approximately 500 to 2000 ion pairs per cm^3 under fair weather conditions [3]. The atmosphere is electrically stratified. Small ions, produced primarily by cosmic radiation, radioactive emanation from the ground, and solar ultraviolet ionisation, are the principal charge carriers for near surface conduction

[3], [4]. The MPI Engine concept theoretically investigates whether this naturally occurring distributed atmospheric charge environment may contribute to plasma assisted propulsion processes when combined with active ionization and electromagnetic acceleration systems [3], [4], [5], [6].

2.2 Atmospheric Ion and Plasma

Charge concentration at sharp conductive points follows from Gauss's law i.e. the surface electric field is inversely related to the local radius of curvature. When the enhanced field near a sharp conductor exceeds the dielectric breakdown threshold of air (approximately 3 MV/m at standard conditions), corona discharge occurs, producing a localised stream of ions and free electrons [3], [4]. The MPI infrastructure exploits this principle through arrays of pointed carbon based "energy nail" and "energy fibre" structures on Ringway pillars and vehicle surfaces, creating a localised high density "energy cloud" that serves as the ion intake zone [1], [2], [4].

2.3 The Corona Effect and Field Enhancement

When a conductor carries a sufficient charge, the local electric field at its surface is given by Gauss's law: E_surface = σ/ε_0, where σ is the surface charge density and ε_0 is the permittivity of free space. For a conductor with high surface curvature (sharp tip, radius r), the local field scales approximately as $E \propto 1/r$, so that very sharp points sustain fields orders of magnitude higher than a flat surface carrying the same total charge [3].

$$E_tip \approx V / (r \cdot \ln(R/r)) \qquad (2.1)$$

where V is the applied or ambient potential, r is the tip radius, and R is a characteristic system dimension. When E_tip exceeds the dielectric breakdown threshold of air (~3 MV/m at standard conditions, 20 °C, 1 atm), corona discharge is initiated: electrons are accelerated in the high field region, collide with neutral molecules, and produce an avalanche of ion pairs [3]. The resulting localised ion enriched volume and the energy cloud is the primary ion source for the MPI Engine intake [2], [4]. In positive corona (anode side), streamers propagate outward from the tip and positive ions drift into the bulk gas. In negative corona (cathode side), Trichel pulses generate regular bursts of negative ions that drift outward. The MPI system exploits both polarities: positive and negative ions are collected simultaneously and separated electromagnetically inside the reactor [2], [6].

2.4 Lorentz Force and Electromagnetic Acceleration

The fundamental equation governing ion motion in the MPI Engine is the Lorentz force law:

$$F = q(E + v \times B) \qquad (2.2)$$

where q is the ion charge, E is the electric field, v is the ion velocity, and B is the magnetic flux density. For a plasma with current density J in magnetic field B, the bulk electromagnetic body force density is:

$$f = J \times B \qquad (2.3)$$

The J × B (Lorentz) term dominates in the magnetic acceleration zone of the MPI Engine, transferring directed momentum to the plasma exhaust [5], [6]. This is the same mechanism employed in magnetoplasmadynamic (MPD) thrusters for in space propulsion but applied here to a predominantly atmospheric working fluid operating at near sea level pressures rather than in vacuum [5], [6].

2.5 Electrostatic Ion Acceleration and Specific Impulse

In the electrostatic acceleration stage, ions of charge e and mass m_i are accelerated through a net grid potential V_acc. Conservation of energy gives the exhaust velocity:

$$v_e = \sqrt{(2eV_{acc} / m_i)} \quad (2.4)$$

To sustain a sufficiently dense plasma in the reactor housing, charged particles must be confined long enough to complete the ionisation and acceleration cycle. The MPI Engine can employ a magnetic mirror (magnetic bottle) geometry: a region of relatively weak field B_0 at the centre flanked by regions of stronger field B_max at each end [6]. Particles with pitch angle θ satisfying:

$$\sin^2\theta_{loss} = B_0 / B_{max} \quad (2.5)$$

are confined; those with smaller pitch angles escape through the loss cone. The mirror ratio R = B_{max}/B_0 determines confinement effectiveness.

Charged particles follow helical trajectories with gyroradius:

$$r_L = mv_\perp / (qB) \quad (2.6)$$

where $v_\perp$ is the velocity component perpendicular to B.

Supplementary ionisation can be achieved by radiofrequency (RF) power deposition at 13.56 MHz, the standard industrial ISM frequency. The volumetric power deposition is:

$$P_{RF} = \iiint (\sigma/2)|E|^2 \, dV \quad (2.7)$$

where σ is the plasma conductivity and E is the RF electric field amplitude [4]. At moderate plasma densities ($n_e \sim 10^{16}$–10^{18} m^{-3}), the collisional ionisation rate coefficient $\langle \sigma_i v_e \rangle$ (averaged over the Maxwellian electron velocity distribution) is approximately 10^{-14} m^3/s at electron temperature T_e = 5 eV, giving volumetric ionisation rates of $R_i = n_e n_n \langle \sigma_i v_e \rangle \sim 10^{18}$–$10^{20}$ $m^{-3}s^{-1}$.

3. Magnetoplasmaionic (MPI) Engine

3.1 Magnetoplasmaionic (MPI) Engine Overview

The MPI Engine integrates six functional subsystems in series: (1) atmospheric energy collection and ion gathering, (2) intake and compression, (3) ionisation chamber, (4) electromagnetic ion separation, (5) magnetic confinement and acceleration chamber, and (6) magnetic nozzle and exhaust [2], [6]

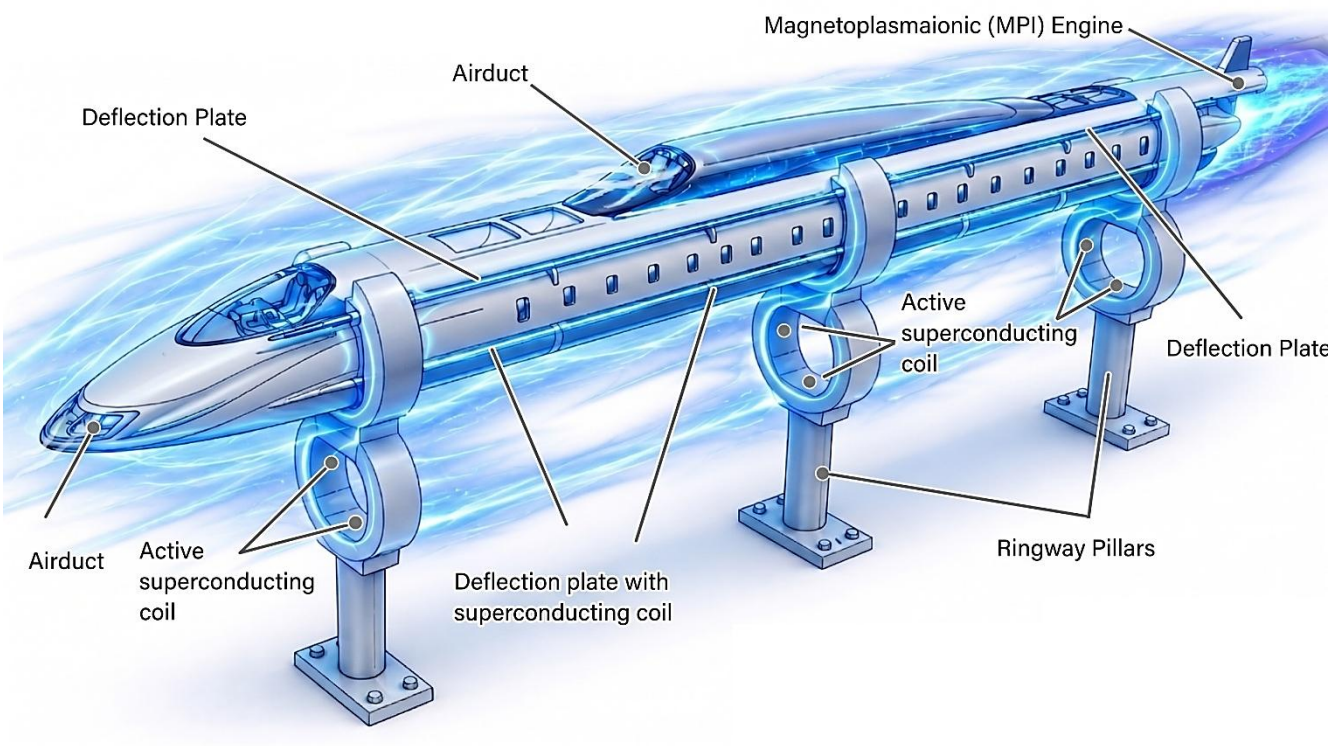


Figure 1 is a conceptual layout of the MPI Engine showing atmospheric energy collection on pillars, ions injection air duct, MPI Engine at rear end [1], [3], [2].

3.2 Atmospheric Energy Collection

Arrays of pointed carbon based energy nail and energy fibre structures are mounted on Ringway infrastructure pillars and on the vehicle nose and upper surface. These structures exploit the geometry dependent field enhancement to intensify the ambient atmospheric electric field at their tips, initiate positive and negative corona discharges, and accumulate a localised energy cloud of ions and electrons in the passage through which each vehicle travels [3], [4]. The effective ion collection current I_col depends on the ambient electric field E_atm, wind speed v_wind, humidity H, tip geometry, and the number density of collection structures per unit pillar height [3], [4]:

$$\eta_{col} = I_{col} / I_{avail} = f(E_{atm}, v_{wind}, H, geometry) \quad (3.1)$$

where I_avail is the available atmospheric ion current. In practice, η_col is expected to range from a few percent under calm fair weather conditions to potentially 20–40% in the vicinity of embedded thunderstorm systems where local ion densities are 10 to 100× the fair weather background [3]. Carbon fibre and graphene are the preferred energy nail and energy fibre materials because, at the microscopic level, graphene and graphite surfaces present an extremely high density of atomic scale sharp points each acting as an independent corona site providing a large effective collection area per unit mass [2], [4]. The collected charge is routed through rectifier diodes (to prevent reverse discharge) and stored in onboard high voltage capacitors before being supplied to the Engine Propulsion Control Unit (EPCU) [2].

3.3 Air Intake, Filtration, and Compression

A nacelle profile, electrically non conductive air duct is mounted at the front upper surface of the vehicle, aligned with the vehicle's axis of travel. The aerofoil front structure channels the incoming airflow and co-captured ion mixture into the duct and toward the reactor housing [2]. The intake may

incorporates:
Particulate filtration: a multistage electrostatic and mesh filter removes dust, water droplets, and foreign particles that could damage the electrode surfaces.
Compression stage: a compressor increases the density of the inlet gas upstream of the ionisation chamber, increasing collisional ionisation efficiency by raising the neutral-particle number density n_n.
Electromagnetic pre-ioniser: an optional high frequency electromagnetic pre-ioniser stage increases ionisation degree before the gas enters the main reactor housing, reducing the ionisation power required from the primary RF and electron bombardment stages [2], [4].

3.4 Ionisation Subsystem

The ionisation chamber converts the filtered, compressed neutral atmospheric gas into a high-density plasma using two complementary mechanisms operating simultaneously:

Mechanism 1 Electron Impact Ionisation:

High energy electrons (emitted by the neutraliser cathode coil) collide with neutral gas molecules M:

$$e^- + M \rightarrow M^+ + 2e^- \qquad (3.2)$$

The electron impact ionisation rate is:

$$R_i = n_e \cdot n_n \cdot \langle \sigma_i(v_e) \cdot v_e \rangle \qquad (3.3)$$

where n_e is the electron number density (m^{-3}), n_n is the neutral density (m^{-3}), σ_i is the ionisation cross section, and <σ_i v_e> is the rate coefficient averaged over the electron velocity distribution [3], [4].

Mechanism 2 Radiofrequency (RF) Ionisation:

RF power at 13.56 MHz is inductively coupled into the plasma via an external coil surrounding the reactor housing. The oscillating electromagnetic field heats electrons to T_e = 3–10 eV, sufficient to drive efficient impact ionisation of nitrogen, oxygen, argon, and xenon. The RF heating also sustains the plasma against recombination losses during the confinement phase [3], [6].

Following ionisation, an electromagnetic ion separation reactor applies a transverse unidirectional magnetic field to the ion mixture. Positive and negative charge species undergo E×B drift in opposite directions, allowing them to be routed separately into the main confinement chamber or exhausted [2], [5].

3.5 Electromagnetic Ion Separation

When a magnetised plasma containing both positive ions and electrons is subjected to a unidirectional transverse magnetic field B_sep, the ion beam acquires self polarisation: the lighter electrons deflect more readily than the heavier ions, producing a net space charge electric field across the beam. This field is exploited to route the positive ions toward the main accelerator grids while the residual electrons are directed to the beam neutralisation region downstream. The degree of separation is governed by the ratio of the E×B drift velocity to the thermal velocity of each species.

3.6 Superconducting Magnetic Confinement

MPI Engine may have six superconducting solenoid coils wound from YBCO (yttrium barium copper

oxide) tape conductors and may be operated at 77 K with liquid nitrogen cooling, generate the magnetic bottle confinement geometry [6], [2], [7]. The axial field profile along the principal axis is approximated by:

$$B_z(z) = B_0 [1 + (z/L)^2] \quad (3.4)$$

where B_0 is the minimum field strength range of (0.1–0.5 T) at the midplane and L is a characteristic mirror length. This profile provides the converging diverging magnetic bottle needed to confine plasma and to focus the accelerated exhaust [2], [5], [6] . Individual coil currents be regulated by closed loop Hall effect magnetic field sensors at 50 kHz sampling rate, maintaining field uniformity within ±2% across the plasma volume. Quench protection circuits including resistive shunts and voltage tap monitors are integrated in each coil to prevent thermal runaway of the YBCO conductor [6], [7], [8].

3.7 Electromagnetic Acceleration and Magnetic Nozzle

In the acceleration region, the J × B Lorentz body force acts on the plasma current interacting with the applied axial magnetic field, accelerating plasma in the exhaust (aft) direction [5], [6]. The electrostatic accel-decel grid system consisting of a positively biased screen electrode, a grounded second screen, and a negatively biased accelerator electrode provides the primary electrostatic acceleration potential V_acc. Exhaust velocity follows Equation (2.4). The converging magnetic nozzle downstream of the last coil focuses and directs the plasma exhaust. Asymmetric current distribution in the nozzle coil allows ±5° thrust vectoring for lateral stability augmentation. The total MPI thrust is given by the thrust equation:

$$F = \dot{m} \cdot v_e + (p_e - p_a) \cdot A_e \quad (3.5)$$

where ṁ is the propellant mass flow rate (kg/s), p_e and p_a are exhaust plane and ambient static pressures (Pa), and A_e is the nozzle exit area (m²). At near atmospheric ambient pressure, the pressure thrust term (p_e − p_a)·A_e is small relative to the momentum thrust ṁ·v_e, so momentum thrust dominates [5].

A neutraliser cathode port immediately downstream of the accelerator grids injects electrons into the exhaust beam to neutralise residual positive charge, producing a quasi-neutral exhaust plume and preventing spacecraft charging analogue effects on the vehicle structure [2], [5].

4. Configuration of Magnetoplasmaionic (MPI) Engine

4.1 Key components of MPI Engine

The MPI Engine comprises primary hardware configuration components [2]. Each component is described below with its function, geometry, and interface within the overall engine assembly. A conceptual assembly of MPI Engine is referred to in figure 2.

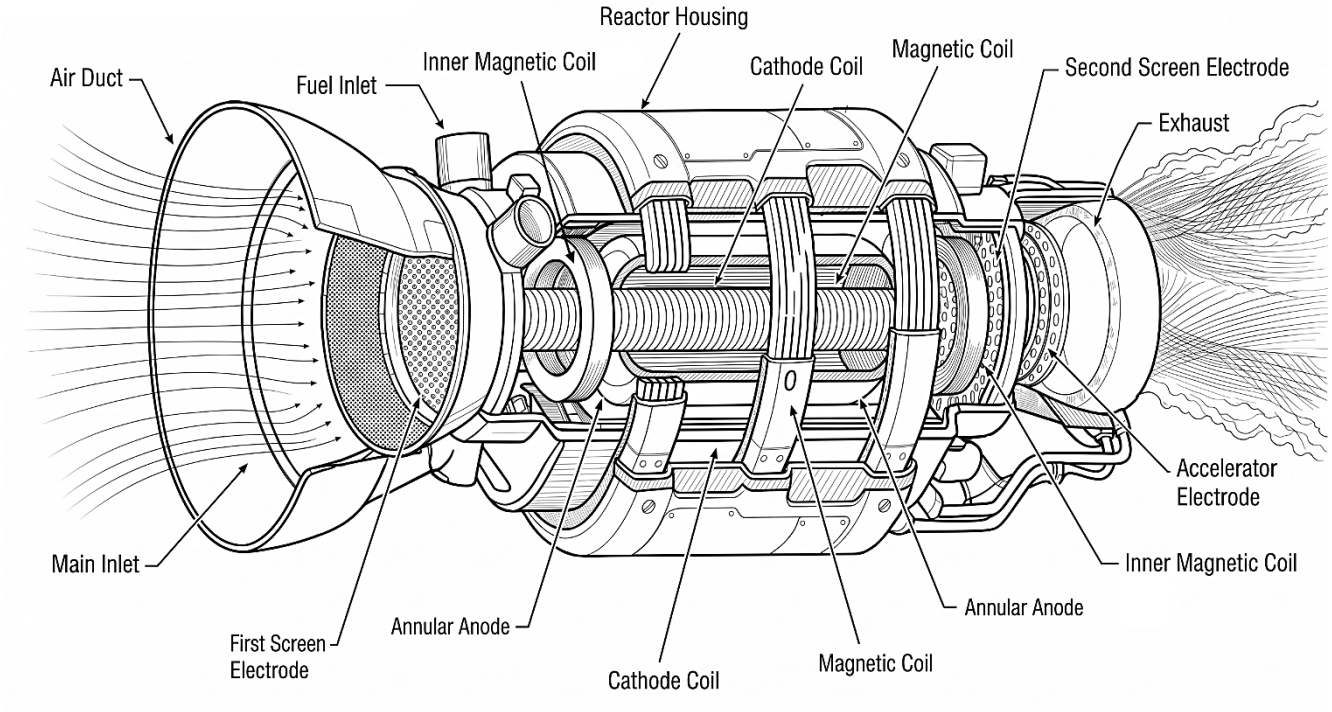


Figure 2 illustrates the configuration of Magnetoplasmaionic (MPI) Engine [2].

4.1.1 Air Duct

Air Duct is nacelle profile, electrically non-conductive duct mounted on the upper forward surface of the vehicle. The non-conductive material (e.g. PTFE, high-temperature polymer composite, or ceramic composite) prevents static charge accumulation that could discharge into the intake flow and disrupt the ion mixture. The nacelle shape minimises pressure drag at high speed while maximising mass-flow capture. Internal guide vanes direct the incoming ion gas mixture toward the pre-filtration and compression stages. Atmospheric ions enter MPI engine via air duct through main inlet [1], [2], [4].

4.1.2 Reactor Housing

Reactor Housing is a cylindrical pressure vessel with a nozzle shaped aft section aligned with the principal axis of the engine. The housing provides: (i) structural containment of the high pressure ionised gas; (ii) electromagnetic shielding of internal components; (iii) thermal isolation between the hot plasma core and the superconducting coils on its exterior. Candidate materials include refractory metals (tungsten, molybdenum) for inner plasma facing surfaces and structural steel or titanium alloy for the outer pressure shell [2].

4.1.3 Cathode Coil

Cathode Coil act as Neutraliser Cathode is centrally located, coaxial coil whose axis coincides with the reactor housing principal axis. Functions dually as: (i) the primary electron emitter for electron bombardment ionisation of the incoming gas; and (ii) the beam neutraliser, injecting electrons into the accelerated positive ion beam to produce a quasi-neutral exhaust plume. The cathode coil is wound from high temperature refractory wire (tungsten) and is sustained by a secondary cathode discharge [2], [5].

4.1.4 Annular Anode

Annular Anode coaxially surrounds the cathode coil inside the reactor housing, maintained at a positive

potential relative to the cathode. The anode–cathode potential difference drives the bombardment discharge and sustains the electron circulation required for efficient ionisation. Azimuthal symmetry of the annular geometry ensures uniform radial ionisation of the incoming gas stream [2], [4].

4.1.5 External Magnetic Coil

External Magnetic Coil is wound around the outside of the reactor housing wall, producing an approximately constant axial magnetic field with flux lines parallel to the principal axis. This field: (i) causes electrons to spiral in helical paths, extending their path length through the neutral gas and increasing ionisation collisions; (ii) constrains electrons from drifting directly to the inner anode surface, reducing electron loss and maintaining high ionisation efficiency; (iii) provides the bulk of the axial confinement field for the magnetic bottle geometry [2], [6].

4.1.6 Inner Magnetic Coil

Inner Magnetic Coil is positioned at each end of the reactor housing; produces an increased magnetic field at the mirror ends, bending field lines inward to confine plasma and prevent axial loss. Can be implemented by increasing winding density, increasing coil current, or overlapping with the external coil windings. Also initiates the converging magnetic nozzle field geometry [2], [5].

4.1.7 Fuel Inlet Port

Fuel Inlet Port is dedicated injection channel for onboard inert propellant (typically xenon, but argon or krypton may also be used). In Sonic Mode, xenon flow is metered by the EPCU controlled propellant management valve. The port injects propellant co axially to mix with the atmospheric ion stream upstream of the ionisation chamber [2].

4.1.8 Main Inlet

Main Inlet is primary entry aperture at the upstream end of the reactor housing through which the combined atmospheric ion–gas mixture (and, in Sonic Mode, propellant) enters the ionisation chamber. The main inlet geometry is optimised to minimise turbulence while maximising mass flow uniformity across the reactor cross section [2].

4.1.9 First Screen Electrode

First Screen Electrode is an open metallic wire/member screen at the upstream (main inlet) end of the acceleration stage. Maintained at positive potential (first polarity) to repel incoming positive ions and to attract electrons from the cathode, facilitating ionisation in the inter electrode space. Configured with sufficient porosity (square, rectangular, or circular apertures) to allow easy passage of the ion gas mixture while providing adequate surface area for charge application [2].

4.1.10 Second Screen Electrode

Second Screen Electrode is an open metallic wire/member screen near the downstream end, maintained at positive potential. Works in concert with the first screen to sustain the ionisation region. Also acts as the extraction plane for the positive ions, channelling them toward the accelerator electrode [2], [5].

4.1.11 Accelerator Electrode

Positioned immediately downstream of the second screen electrode, maintained at negative potential (second polarity, accel-decel scheme). Strongly attracts positively charged ions and accelerates them through the exhaust egress to generate thrust. The accel-decel arrangement upstream screen positive, accelerator negative provides higher beam density at a given net voltage and reduces

electron backstreaming from the neutralised downstream beam. Grid perforations are analytically configured to focus the ion beam with minimum electrode impingement [2], [5].

4.1.12 Exhaust

Aft egress section where accelerated ions exit at high velocity to generate thrust. The exhaust section geometry transitions from the cylindrical reactor housing to the magnetic nozzle profile, providing controlled divergence of the exhaust plume. The body of the vehicle tapers aft of the exhaust egress to prevent interaction of the hot exhaust plume with the vehicle structure [2].

5. MPI Engine Integration with Ringway Transportation System

5.1 Ringway Transportation System Overview

The Ringway Transportation System is a novel high capacity, high speed guideway in which vehicles travel through a succession of ring shaped frames mounted on vertical pillars at regular spacing. The system differs fundamentally from conventional rail in that: (i) the vehicle is completely enclosed by the ringway frame at each pillar, providing passive structural containment in the event of derailment; (ii) the guideway is elevated above existing surface infrastructure, eliminating grade level conflicts; (iii) both maglev levitation and MPI propulsion exploit the same electromagnetic infrastructure; and (iv) atmospheric energy collection is passive and continuous regardless of vehicle operation [1], [2].

5.2 Mode of Operation

The MPI Engine is designed to operate in three distinct modes, each representing a different combination of active subsystems, propellant sources, and performance envelope. Mode selection is governed by the supervisory Central Control Unit (CCU), which continuously monitors vehicle speed, available atmospheric ion density, onboard propellant inventory, guideway state, and safety conditions [1], [2]. In this paper, sonic mode is discussed in detail. Sonic Mode activates all MPI subsystems simultaneously: dual engine configuration (if fitted), maximum atmospheric ion collection, full RF ionisation, maximum xenon propellant injection, and full energisation of all superconducting coils and electrode screens. This mode targets supersonic speeds on the near frictionless maglev guideway, with indicative operating speeds of 600 to 1,200 km/h [1], [2].

The Sonic Mode force balance on the vehicle is:

$$F_{lateral} = 0; \quad F_{MPI} + F_{mag} - F_{aero} - F_{drag} = m \cdot a \tag{5.1}$$

where F_MPI is total MPI thrust, F_mag is the LSM propulsion force, F_aero is aerodynamic resistance, F_drag is guideway rolling/friction resistance, m is vehicle mass, and a is longitudinal acceleration. Lateral force balance is maintained by the superconducting maglev guidance system [7], [8].

5.3 Pillar and Ringway Vehicle Structural Design

Each Ringway pillar is an independent structural column founded on a base extending to maximum depth appropriate to local soil and seismic conditions. The pillar spacing equals or always exceeds the vehicle body length so that the vehicle is supported by at least two pillars simultaneously. The pillar carries: (i) the ring shaped Ringway frame on pillars; (ii) the mechanical roller assembly for emergency/low speed guidance; (iii) the superconducting LSM propulsion coil windings; and (iv) the atmospheric energy collection subsystem (energy nail and energy fibre arrays, diodes, capacitors, and wiring) [1], [2]. The ring frame geometry provides a passive safety barrier: if the vehicle loses maglev levitation and deflects laterally, the deflection plate cage contacts the mechanical rollers of

the frame, converting a potentially catastrophic derailment into a controlled deceleration slide [1], [2]. This is a fundamental safety advantage over open guideway maglev systems where derailment has no structural containment.

5.4 Deflection Plate Interface

The vehicle body carries deflection plates on all four sides (lateral, vertical-upper, vertical-lower, and longitudinal-fore and aft), mounted on articulated bogies with air-spring suspension. The deflection plate serves three simultaneous functions: (i) as the reaction surface for superconducting maglev modules providing levitation and guidance forces; (ii) as the engagement surface for mechanical rollers at stations, low-speed segments, and emergency contact; and (iii) as the structural interface between the vehicle fuselage and the bogie assembly that transmits propulsion loads from the LSM. Each deflection plate incorporates: a minimum of two fore-and-aft flexion joints to accommodate thermal expansion and guideway curvature; a coolant tube network to maintain surface temperature within the operating range of the superconducting modules; and a lubrication distribution system to reduce friction when mechanical roller contact occurs [1], [2].

5.5 Maglev System

Superconducting permanent magnet modules (YBCO based) mounted on the vehicle deflection plates interact with iron-cored long-stator linear synchronous motor (LSM) windings embedded in the Ringway frame structure to provide: (i) electromagnetic levitation (EDS/EMS hybrid); (ii) lateral guidance through null-flux coil arrays; and (iii) primary longitudinal propulsion through three phase LSM excitation [1], [2], [7], [8].

6. Aerospace Application

6.1 Low Altitude Atmospheric Aircraft

In low altitude atmospheric flight (0 to 3,000 m), ion concentrations are highest, the atmospheric electric field is strongest, and the MPI Engine's atmospheric feedstock advantage is most pronounced. Aircraft mounted MPI units could provide supplementary thrust or energy recovery during cruise, reducing fuel consumption of the primary propulsion system. The denser near surface environment increases the achievable collection current I_col by a factor of 2 to 5× relative to sea level fair weather conditions in the presence of nearby convective weather systems [3], [4]. For unmanned aerial vehicles (UAVs) operating persistently in the atmospheric boundary layer, MPI energy collection could support auxiliary electrical loads (avionics, sensors, communications), extending endurance without increasing onboard battery mass. The continuous atmospheric ion production by cosmic rays and radioactivity ensures a baseline ion supply independent of local weather [3], [4].

6.2 Hypersonic Re-entry Vehicle

At hypersonic speeds at Mach 5+, aerodynamic heating creates a high enthalpy plasma sheath around the vehicle forebody. MPI type electromagnetic concepts may offer a theoretical basis for interaction with hypersonic plasma sheaths; however, practical energy recovery remains an open research question and redirect it to provide additional propulsive thrust, a concept analogous to energy recovery in regenerative braking [2], [5]. The Lorentz force acceleration mechanism (J × B) is directly applicable to the hypersonic plasma environment.

7. Summary and Conclusion

This paper has presented a comprehensive conceptual design study of the Magnetoplasmaionic

(MPI) Engine, a novel propulsion architecture that integrates atmospheric ion harvesting, staged plasma ionisation, superconducting magnetic confinement, and Lorentz-force electromagnetic acceleration into a single engine system. The concept was developed as the primary longitudinal propulsion element of the Ringway Transportation System [1], [2] but its underlying physical principles are sufficiently general to inform future low altitude aircraft, hypersonic vehicle, and maritime propulsion research [1], [2], [5], [6]. The subsystem architecture atmospheric collection, intake/compression, ionisation, electromagnetic separation, magnetic confinement, and magnetic nozzle acceleration is described at the component level through the twelve primary hardware items of the patent specification [1], [2].

8. Contact Author Email Address

naveenkumarchaudhary@outlook.com

9. Copyright Statement

The authors confirm that they, and/or their company or organization, hold copyright on all the original material included in this paper. The authors also confirm that they have obtained permission, from the copyright holder of any third-party material included in this paper, to publish it as part of their paper. The authors confirm that they give permission or have obtained permission from the copyright holder of this paper, for the publication and distribution of this paper as part of the ICAS proceedings or as individual off-prints from the proceedings.

References

[1] N. K. Chaudhary[1], "Improvement in Mass Transportation," Patent No. IN352291, 2012.
[2] N. K. Chaudhary[1], “An elongated gliding vehicle and high-speed transportation system,” Patent No. IN533273, 2020.
[3] V. Y. Kozhevnikov et al., "Key Modes of Ignition and Maintenance of Corona Discharge in Air," Energies, vol. 16, no. 13, p. 4861, 2023.
[4] T.-Y. Wen et al., "Corona discharge characteristics of cylindrical electrodes in a two-stage electrostatic precipitator," Heliyon, vol. 6, p. e03334, 2020.
[5] G. Coppola et al., "Low-Power Magnetoplasmadynamic Thruster Numerical Performance Model," Applied Sciences, vol. 16(9), 2026.
[6] A. S. Voronov et al., "Magnetoplasmadynamic thruster with an applied field based on the second generation high-temperature superconductors," Journal of Physics: Conference Series, vol. 1686, p. 012023, 2020.
[7] C. Zhang et al., "Modelling, Optimisation, and Construction of a High-Temperature Superconducting Maglev Demonstrator," Machines, vol. 14, no. 1, art. 108, 2026.
[8] O. Vakaliuk et al., "A multifunctional highway system incorporating superconductor levitated vehicles and liquefied hydrogen," APL Energy, vol. 1, no. 1, p. 016107, 2023.